9

Laminar Mixed Convection Heat and Mass Transfer with Phase Change and Flow Reversal in Channels

Brahim Benhamou[1], Othmane Oulaid[1,2],
Mohamed Aboudou Kassim[1] and Nicolas Galanis[2]
[1]*LMFE, CNRST-URAC27, Cadi Ayyad University, Marrakech,*
[2]*Mechanical Eng. Department, Université de Sherbrooke, Sherbrooke,*
[1]*Morocco*
[2]*Quebec, Canada*

1. Introduction

Due to its widespread applications, heat and mass transfer in an air stream with liquid film evaporation or condensation in open channels has received considerable attention in the literature. This kind of flows is present in many natural and engineering processes, such as human transpiration, desalination, film cooling, liquid film evaporator, cooling of microelectronic equipments and air conditioning.

Since the original theory for flow of a mixture of vapour and a non-condensable gas by Nusselt (1916) and its extension by Minkowycz & Sparrow (1966), many theoretical and experimental studies have been published in the literature. These studies deal with different geometric configurations such as a flat plate, parallel-plate channel and rectangular or circular-section ducts.

Heat and mass transfer convection over a flat plate wetted by a liquid film has been investigated by Vachon (1979). He performed an analytical and experimental study of the evaporation of a liquid film streaming along a porous flat plate into a naturally driven airflow. This author established correlations for Nusselt and Sherwood numbers in connection with a combined Grashof number. Ben Nasrallah & Arnaud (1985) investigated theoretically film evaporation in buoyancy driven airflow over a vertical plate heated with a variable heat flux. The solutions of the governing equation have been obtained by means of semi-analytical and finite difference methods. The authors present their results in term of expressions of the wall temperature and mass fraction as well as the local Nusselt and Sherwood numbers. A numerical and experimental analysis has been carried out by Tsay et al. (1990) to explore the detailed heat transfer characteristics for a falling liquid film along a vertical insulated flat plate. Free stream air temperature was set at 30°C and inlet liquid film temperature was taken equal to 30°C or 35°C. The results show that latent heat transfer connected with vaporization is the main cause for cooling of the liquid film. The authors affirm that when the inlet liquid temperature is equal to the ambient one, latent heat transfer due to the film vaporization initiates heat transfer in the film and gas flow. Aguanoun et al (1994; 1998) studied numerically the evaporation of a falling film on an inclined plate heated

at a constant temperature in a humid air stream. They considered forced (Agunaoun et al., 1994) or mixed convection (Agunaoun et al., 1998) with several liquid mixtures. A boundary layer type model was adopted. The authors stated that the liquid film-gas interface has approximately the same temperature as the plate in the case of forced convection.

Yan & Soong (1995) considered turbulent heat and mass transfer convection over a wetted inclined plate. The liquid film flow is turbulent and waves less. Their results pointed out that the plate and the gas-liquid interface temperatures are reduced consequently to the increase of the plate's inclination angle, the inlet film thickness or the air velocity. Mezaache & Daguenet (2000) conducted a numerical study of the evaporation of a water film falling on an inclined plate in a forced convection flow of humid air. The plate is insulated or heated by a constant heat flux. The main result of this study was that the enthalpy diffusion term in the energy equation does not influence the film temperature. This term represents the effect of the species diffusion on enthalpy of the humid air mixture. Volchkov et al. (2004) reported a numerical work on both laminar and turbulent forced convection of humid air over an infinite flat plate. The authors aim to establish the validity of the heat-mass transfer analogy. The steam in the humid airflow may condense on the plate whose temperature is lower than that of the airflow. The authors made a major simplification by neglecting the effect of the condensate film. This assumption is justified by the experimental data in the literature which indicate that measurements of the liquid film-air interface temperature in humid-air flows show that it is close to the saturation temperature corresponding to the vapour concentration at the plate. This point is addressed hereafter. Recently, Maurya et al. (2010) developed a numerical analysis of the evaporating flow of a 2-D laminar, developing film falling over an inclined plate, subjected to constant wall heat flux. Their results show that the evaporation process begins only after the growing thermal boundary layer reaches the interface.

Heat and mass transfer in a vertical heated tube with a liquid film falling on its inside walls was treated by Feddaoui et al. (2003). They considered co-current downward flows of liquid water and humid air. The airflow is turbulent while the liquid one is laminar and without surface waves. The authors concluded that better cooling of the liquid film is obtained for higher heat flux or lower inlet liquid flow. Lin et al (1988) analysed numerically combined heat and mass buoyancy effects on laminar forced convection in a vertical tube with liquid falling film. Their results show that large film evaporation rates are obtained for larger tube wall temperature. Convective instability of heat and mass transfer for laminar forced convection in the thermal entrance region of a horizontal rectangular channel has been examined by Lin et al. (1992). The rectangular channel is thermally insulated except for the bottom wall. The latter is maintained at a constant temperature and covered by a thin liquid water film. The thickness of this film is neglected, thus it is treated as a boundary condition for heat and mass transfer. Inlet air temperature was fixed at 20°C. The effects of changes of bottom wall temperature, relative humidity of air at the entrance and the channel aspect ratio are examined. The results show that the convective instability is affected by changes in inlet air relative humidity and temperature and also the channel aspect ratio. Huang et al. (2005) conducted a numerical study on laminar mixed convection heat and mass transfer in a rectangular duct. Two of the duct walls were wetted by a thin liquid water film and maintained at different constant temperatures. The other walls are insulated. Air entered the duct with a constant temperature lower than that of the walls. The authors established that vapour condensation occurred on the wall with lower temperature.

Nelson & Wood (1989) studied the developing laminar natural convection flow in a vertical parallel-plate channel. They used a boundary-layer approximation model to derive a

correlation for the heat and mass transfer coefficients in the case of uniform temperature and concentration plates. Yan and co-workers (Yan et al. 1989; Yan & Lin, 1989; Tsay et al. 1990, Yan et al. 1990; Yan 1991; Yan & Lin 1991; Yan et al. 1991; Yan 1993; Yan 1995a; Yan 1995b) investigated the influences of wetted walls on laminar or turbulent mixed convection heat and mass transfer in parallel-plate channels. Constant wall temperature, constant wall heat flux or insulated walls were considered. All of these numerical works were conducted with a boundary-layer type mathematical model. The results of these studies showed that the effects of the water film evaporation on the heat transfer are rather substantial. Two-phase modelling of laminar film condensation from mixtures of a vapor and a non-condensing gas in parallel-plate channels has been studied by Siow et al. (2007). The channel is inclined downward from the horizontal and has an isothermal cooled bottom plate and an insulated upper one. Results for steam-air mixtures are presented and the effects of changes in the angle of inclination, inlet gas mass fraction, airflow Reynolds number and inlet temperature are examined. It was found that an increase in the angle of inclination results in thinner and faster moving liquid films. The authors show that, increasing airflow Reynolds number always produced thinner films and higher Nusselt number.

One of the main matters of the considered problem is the liquid film modelling. Many simplifying assumptions were used in the literature to derive mathematical models for the liquid phase. The boundary layer approximations are often used to derive a simplified model (Chow & Chung 1983; Chang et al. 1986; Lin et al. 1988; Yan & Lin 1989; Yan et al. 1989; He et al. 1998; Mezaache & Daguenet 2000).

Regarding the liquid-gas interface, one of the main hypotheses used in the literature is the so-called Nusselt's approximation (Nusselt, 1916), which neglects the shear stresses along this interface (Suzuki et al. 1983; Shembharkar & Pai 1986; Baumann & Thiele 1990). On the other hand, for accurate estimation of the evaporation process at the liquid-gas interface Maurya et al. (2010) used a numerical model that couples the Volume Of Fluid (VOF) method and the Ghost Fluid Technique (GFT). The VOF conservation method permits the interface tracking, while the GFT enables the authors to implement the interfacial condition (i.e. the prescription of saturation temperature) and the accurate estimation of temperature gradients on either side of the interface. This technique gives a more accurate estimation of the temperature gradients at the wall (and, hence, the heat transfer coefficient) than Nusselt's theory, which ignores the inertial effects.

An interesting way to deal with the liquid film modelling was used by some authors (Lin et al. 1988; Yan 1993; Fedorov et al. 1997; Volchkov et al. 2004; Huang et al. 2005; Azizi et al. 2007; Laaroussi et al. 2009; Oulaid et al. 2010b). These authors assumed an extremely thin liquid film so that it could be treated as a boundary condition. The validity of this assumption has been investigated by Yan (1992; 1993) for both air-water and air-ethanol systems. The author conducted a study of laminar mixed convection with evaporation of a liquid film dripping on the inner walls of a vertical channel. The walls are isothermally heated (Yan, 1993) or heated by a uniform heat flux (Yan, 1992). In each case the author conducted two studies: one with the conservation equations solved both in liquid and gas phases and in the other the film thickness was neglected. By comparing the results of these two studies, the author was able to demonstrate that the assumption of negligible film thickness is valid for low liquid film flow rates.

Many authors assumed constant thermo-physical properties evaluated at a reference temperature T_{ref} and mass fraction ω_{ref} obtained by these expressions: $T_{ref} = (2.T_w + T_{in})/3$ and $\omega_{ref} = (2.\omega_w + \omega_{in})/3$, where T_w , T_{in}, ω_w and ω_{in} are respectively the channel wall and

inlet air temperatures and mass fractions. This way of evaluating thermo-physical properties, known as the one-third rule, has been used previously in the literature (Hubbard el al. 1975; Chow & Chung 1983). Chow & Chung (1983) performed a numerical study of evaporation of water in a laminar air stream. The water surface temperature was assumed to be constant and equal to the wet bulb temperature of the free stream. Different airflow temperatures were considered (150-500°C). By comparing the results of their models with variable and constant properties evaluated by the one-third rule, the authors concluded that the latter agree well with the variable-property results, even at high airflow temperatures. Earlier, Hubbard et al. (1975) conducted a numerical study on a single droplet evaporation of octane in stagnant air. The initial temperature of the droplet was 27°C and the air temperature was varied in the range 327-1727°C. By comparing their results using various reference property temperatures and concentrations, they concluded that the one-third rule yields the best agreement with the variable-properties model. The validity of the one-third rule for heat and mass transfer problems has been recently checked by Laaroussi et al. (2009). These authors mentioned that the one-third rule remains valid provided that the vapour mass fraction is small.

Flow reversal was studied analytically for fully developed flow with coupled heat and mass transfer by Salah El-Din (1992) and Boulama-Galanis (2004). These authors presented the criteria of occurrence of this phenomenon. These studies are some of the rare ones concerning flow reversal in combined mixed convection heat and mass transfer. On the other hand, flow reversal was extensively studied in thermal convection problems (Nguyen et al., 2004; Wang et al., 1994; Maré et al., 2008; Nesreddine et al., 1998; Faghri et al., 1980; Salah El-Din, 2001). For instance, Nguyen et al. (2004) studied the flow reversal and the instability of a transient laminar thermal mixed convection in a vertical tube subjected to a uniform time-dependent wall heat flux. The problem was investigated numerically by using a full 3D-transient-model and Boussinesq's assumption. The authors showed that the structures of the flow and thermal field appear to remain stable for Gr_T up to 5.0×10^5 and 10^6, respectively, for opposed and assisted-buoyancy cases. Beyond these critical values, the convergence of the numerical scheme becomes extremely slow and tedious. Thus, the authors were enable to point out any flow transition. Mixed convection with flow reversal in the thermal entrance region of horizontal and vertical pipes was studied numerically by Wang et al. (1994). Their results show that, for ascending flow in a vertical pipe, flow reversal is observed at the pipe centre in the heating case (or near the wall in the cooling case) at relatively high |Gr/Re| with constant Péclet number. The regime of flow reversal has been identified for both heating and cooling cases in the Pe-|Gr/Re| coordinates for a vertical pipe and in the Pe-Ra coordinates for heating in a horizontal pipe. Experimental and numerical studies of thermal mixed convection with flow reversal in coaxial double-duct heat exchangers have been carried out by Maré et al. (2008). Velocity vectors in a vertical heat exchanger for parallel ascending flow of water under conditions of laminar mixed convection have been determined experimentally using the particle image velocimetry technique. Their results show that measured velocity distributions are in very good agreement with corresponding numerical predictions and illustrate the simultaneous existence of flow reversal in the tube and the annulus for both heating and cooling of the fluid in the tube. As far as developing flows with heat and mass transfer are concerned, studies on flow reversal are rare (Laaroussi et al. 2009; Oulaid et al. 2010b). Indeed, the majority of the studies on this problem adopted a parabolic model where axial diffusion of momentum, energy and concentration is not taken into account. This model may not be appropriate for flows with low Péclet number where axial diffusion is not negligible (Nesreddine et al., 1998).

The objective of this paper is to summarize some recent work of the authors on heat and mass transfer in parallel-plate channel with phase change with special emphasis on flow reversal.

2. Problem definition and modelling

The physical problem is a parallel-plate channel (Figure 1). Liquid water film flows on the internal faces of these plates, which are maintained at a uniform temperature T_W or thermally insulated. An upward flow of ambient air enters at constant temperature T_0, relative humidity ϕ_0 and uniform velocity u_0. Steady state conditions are considered and the flow is assumed laminar. Radiation heat transfer, the transfer of energy by inter-diffusion of species, viscous dissipation and the work of the compressive forces are considered negligible. The secondary effects of concentration gradient on the thermal diffusion (Dufour effect) and thermal gradient on the mass diffusion (Soret effect) are neglected (Gebhart & Pera, 1971). Finally, the physical properties are assumed to be constant except for the density in the body forces, which is considered to be a linear function of temperature and mass fraction (Oberbeck-Boussinesq approximation),

$$\rho = \rho_0 \left[1 - \beta \left(T - T_0 \right) - \beta^* \left(\omega - \omega_0 \right) \right] \tag{1}$$

The coefficients of thermal and mass fraction expansion, are defined by,

$$\beta_T = \frac{-1}{\rho_0} \left(\frac{\partial \rho}{\partial T} \right)_{\omega=cste,\ p=cste}$$

$$\beta^* = \frac{-1}{\rho_0} \left(\frac{\partial \rho}{\partial \omega} \right)_{T=cste,\ p=cste} \tag{2}$$

As the gas flow considered here is humid air, which is assumed to be a perfect gas, these coefficients are given by,

$$\beta = 1/T_0$$

$$\beta^* = \frac{M_a - M_v}{(M_a - M_v)\omega + M_v} \tag{3}$$

Mass fraction of water vapour in the humid air ω is low, thus the last expression may be simplified as follows

$$\beta^* = M_a/M_v - 1 \tag{4}$$

The Oberbeck-Boussinesq assumption is considered valid for small temperature and mass fraction differences (Gebhart et al., 1988). The validity of this assumption for simultaneous heat and mass transfer was investigated by Laaroussi et al. (2009). These authors compared the Oberbeck-Boussinesq and variable-density models at relatively high temperatures in a vertical parallel-plate channel laminar mixed convection associated with film evaporation.

Their results showed that the Oberbeck-Boussinesq model works well for temperature and mass fraction differences less than 20K and 0.1kg/kg respectively.
The liquid films are assumed to be extremely thin. This hypothesis, known in the literature as the *zero film thickness model*, allows us to handle only the conservation equations in the gas flow with the appropriate boundary conditions. The liquid film is supposed to be at the imposed wall temperature. As reported in the introduction, the *zero film thickness model* is valid for low liquid flow rates (Yan 1992; Yan 1993).
The following non-dimensional variables are defined

$$X = \frac{x}{D_h},\ Y = \frac{y}{D_h},\ U = \frac{u}{u_0},\ V = \frac{v}{u_0},$$

$$P_m = \frac{p_m}{\rho_0 u_0^2},\ \Theta = \frac{T - T_0}{T_W - T_0},\ C = \frac{\omega - \omega_0}{\omega_w - \omega_0} \tag{5}$$

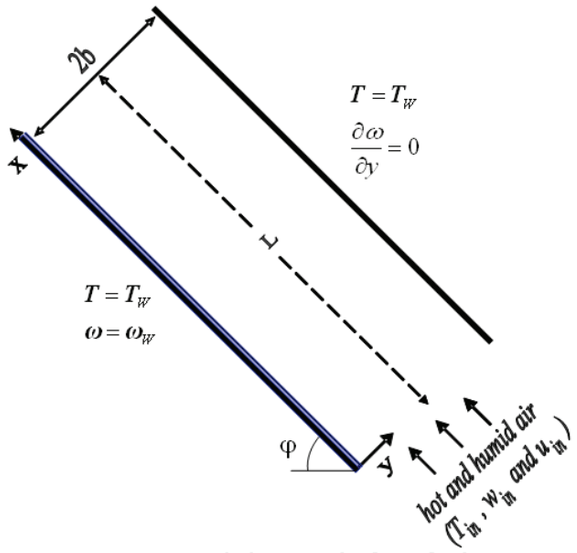

Fig. 1. Sketch of the physical system.

Using these variables and under the above assumptions, the governing equations of the problem are
Continuity equation

$$\frac{\partial U}{\partial X} + \frac{\partial V}{\partial Y} = 0 \tag{6}$$

Stream wise momentum equation

$$\left(U\frac{\partial U}{\partial X} + V\frac{\partial U}{\partial Y}\right) = -\frac{\partial P_m}{\partial X} + \frac{1}{Re}\left(\frac{\partial^2 U}{\partial X^2} + \frac{\partial^2 U}{\partial Y^2}\right) + \frac{\sin\varphi}{Re^2}\left(Gr_T\Theta + Gr_M C\right) \tag{7}$$

Span wise momentum equation

$$\left(U\frac{\partial V}{\partial X}+V\frac{\partial V}{\partial Y}\right)=-\frac{\partial P_m}{\partial Y}+\frac{1}{Re}\left(\frac{\partial^2 V}{\partial X^2}+\frac{\partial^2 V}{\partial Y^2}\right)+\frac{\cos\varphi}{Re^2}\left(Gr_T\Theta+Gr_M C\right) \quad (8)$$

Energy equation

$$\left(U\frac{\partial \Theta}{\partial X}+V\frac{\partial \Theta}{\partial Y}\right)=\frac{1}{Re\,Pr}\left(\frac{\partial^2 \Theta}{\partial X^2}+\frac{\partial^2 \Theta}{\partial Y^2}\right) \quad (9)$$

Species conservation equation

$$\left(U\frac{\partial C}{\partial X}+V\frac{\partial C}{\partial Y}\right)=\frac{1}{Re\,Sc}\left(\frac{\partial^2 C}{\partial X^2}+\frac{\partial^2 C}{\partial Y^2}\right) \quad (10)$$

2.1 Boundary conditions

At the channel inlet (X = 0) the airflow velocity is assumed uniform and in the x-direction with constants temperature and mass fraction,

$$U = 1 \text{ and } V = C = \Theta = 0 \quad (11)$$

At the channel exit (X = 1/2γ), the flow is assumed fully developed. Hence,

$$\frac{\partial U}{\partial X}=\frac{\partial V}{\partial X}=\frac{\partial \Theta}{\partial X}=\frac{\partial C}{\partial X}=0 \quad (12)$$

Four types of conditions on the channel walls are considered here:

- **BC1**: Both of the pates (*Y = 0* and *Y =0.5*) are isothermal and wetted by thin liquid water films.
- **BC2**: The lower pate (*Y = 0)* is isothermal and wetted by thin liquid water films, while the upper one *(Y =0.5*) is isothermal and dry.
- **BC3**: One of the plates (*Y = 0*) is isothermal and wetted by a thin liquid water film while the other (*Y =0.5*) is thermally insulated and dry.
- **BC4**: both of the plates are thermally insulated and wetted by thin liquid water films.

At the insulated and dry plate, the airflow velocity components as well as the temperature and mass fraction gradients are zero. Thus,

$$U = V = 0, \text{ and } \frac{\partial C}{\partial Y}=\frac{\partial \Theta}{\partial Y}=0 \quad (13a)$$

At the isothermal and dry plate,

$$U = 0,\ V = 0,\ \frac{\partial C}{\partial Y}=\frac{\partial \Theta}{\partial Y}=0 \text{ and } \Theta = 1 \quad (13b)$$

At the isothermal and wet plate, the airflow axial velocity is obviously null (no slip) and its transverse velocity is equal to that of the vapour velocity at the liquid-gas interface. The mass fraction is that of saturation conditions at the plate's temperature. Hence,

$$U = 0,\ V = \pm Ve \text{ and } C = \Theta = 1 \quad (13c)$$

At the insulated and dry plate,

$$U = V = 0, \text{ and } \frac{\partial C}{\partial Y} = \frac{\partial \Theta}{\partial Y} = 0 \tag{13a}$$

At the isothermal and dry plate,

$$U = 0,\ V = 0,\ \frac{\partial C}{\partial Y} = 0 \text{ and } \Theta = 1 \tag{13b}$$

At the insulated and wet plate,

$$U = 0,\ V = \pm Ve\ ,\ \frac{\partial \Theta}{\partial Y} = 0 \text{ and } C = 1 \tag{13d}$$

V_e represents the evaporated liquid film into the air stream or condensed humid air vapour on the wet plate. Its non-dimensional form is (Burmeister, 1993)

$$V_e = \frac{-1}{\text{Re Sc}} \frac{(\omega_w - \omega_0)}{(1-\omega_w)} \left(\frac{\partial C}{\partial Y}\right)_{Y=0} \tag{14}$$

The mass fraction at the wall ω_w corresponding to the saturation conditions at T_w, is calculated by assuming that air-vapour mixture is an ideal gas mixture, and its expression is given by:

$$\omega_W = \frac{\frac{M_v}{M_a}}{\frac{M_v}{M_a} + \frac{P}{P_{sat}(T_W)} - 1} \tag{15}$$

2.2 Flow, heat and mass transfer parameters

The friction factor at the channel walls is

$$f.\text{Re} = 2 \left(\frac{\partial U}{\partial Y}\right)_{Y=0, Y=0.5} \tag{16}$$

Heat transfer between the wet walls and the humid air is the sum of a sensible and a latent component flux

$$q'' = q''_S + q''_L = -k \left.\frac{\partial T}{\partial y}\right|_{y=0} - \frac{\rho\ D\ h_{fg}}{1-\omega_w} \left.\frac{\partial w}{\partial y}\right|_{y=0} \tag{17}$$

Therefore, the total local Nusselt number is

$$Nu_T = \frac{h\ D_h}{k} = \frac{q''_T D_h}{k(T_w - T_m)} = Nu_S + Nu_L \tag{18}$$

where

$$Nu_S = -\frac{1}{1-\Theta_m}\frac{\partial\Theta}{\partial Y}\bigg|_{Y=0} \tag{19}$$

$$\mathrm{Nu_L} = -\frac{\rho\, D\, h_{fg}}{k(1-\Theta_\mathrm{m})}\frac{(\omega_w-\omega_0)}{(1-\omega_w)}\frac{1}{(T_w-T_0)}\frac{\partial \mathrm{C}}{\partial \mathrm{Y}}\bigg|_{Y=0} \tag{20}$$

The dimensionless bulk temperature is defined as follows

$$\Theta_m = \frac{1}{U_m}\int_0^{0.5} U\ \ \Theta\ \ dY \tag{21}$$

The Sherwood number characterizes mass transfer at the air-liquid interface

$$Sh = \frac{h_m D_h}{D} = \frac{\dot{m}}{\rho(\omega_W-\omega_m)}\frac{D_h}{D} \tag{22}$$

At the liquid-gas interface the liquid and vapour mass fluxes are equal. This flux, which is due to convective and diffusion transfer, is given by Burmeister (1993)

$$\dot{m} = \rho_\ell v_\ell = \omega_W \rho\ \ \ v_e - \rho\, D\ \frac{\partial\omega}{\partial y}\bigg|_{y=0} \tag{23}$$

For small mass transfer at the liquid-gas interface, as it is the case here, the following expression for Sherwood number is derived (Oulaid et al. 2010b; Huang et al. 2005)

$$Sh = \frac{-1}{(1-C_m)}\ \frac{\partial C}{\partial Y}\bigg|_{Y=0} \tag{24}$$

3. Numerical method

A finite volume method is used for the discretization of the governing equations (Eq. 3-7). The combined convection-diffusion term is calculated with a power-law scheme and an the block-correction method coupled with a line-by-line procedure is used to solve the resulting algebraic equations (Patankar, 1981). The velocity-pressure coupling is treated by the SIMPLER algorithm (Patankar 1980; Patankar 1981). Convergence of this iterative procedure is declared when the relative variations of any dependent variable is less than 10^{-4} and the mass residual falls below 10^{-6} at all the grid points. The grid is non-uniform in both the streamwise and transverse directions with greater node density near the inlet and the walls. Furthermore, different grid sizes were considered to ensure that the solution was grid-independent. Results of the grid sensibility study are given by Ait Hammou et al. (2004) and Kassim et al. (2010). These results show that heat and mass transfer parameters, as well as the local variables, obtained for three grids 100x35, 200x70 and 400x140 vary within less than 5%. Hence, a grid with 100 nodes in the axial direction and 35 nodes in the transverse one is adopted for the results presented here.

Validation of the computer code and the mathematical model has been carried out first for hydrodynamically and thermally developing forced thermal convection (Ait Hammou et al.

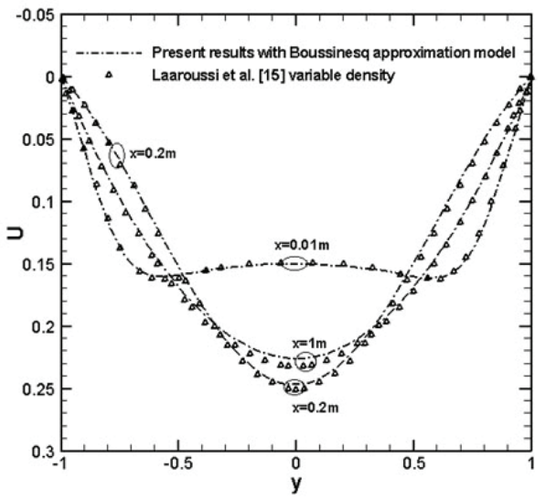

Fig. 2. Comparison between the Oberbeck-Boussinesq model (Oulaid et al. 2010b) and the variable density model (Laaroussi et al., 2009), for $T_W = T_0$=327 K, ω_0=0 and ω_W=0.1.

2004). The results are compared to those obtained by Mercer in the case of a parallel-plate channel with one of the plates isothermal and the other insulated (Kassim et al. 2010)a. Moreover, comparison with the available heat-mass transfer results in the literature for the isothermal wetted parallel-plate channel are satisfactory (Oulaid et al. 2010b).

Figure 2 shows comparison of the velocity profiles obtained by the Oberbeck-Boussinesq model (Oulaid et al. 2010b) and those calculated by the variable-density model (Laaroussi et al., 2009). The discrepancy between the two models is less than 4%.

In view of these successful validations, the computer code, as well as the mathematical model, are considered reliable.

The results presented hereafter are obtained for constant thermo-physical properties evaluated at a reference temperature and mass fraction calculated by the *one-third rule* (Chow and Chung, 1983). As stated in the introduction, this way of evaluating thermo-physical proprieties is believed to be relevant for the present conditions.

4. Uniform wall temperature

In the case of uniform channel walls temperature, both of the plates are subject to the boundary conditions **BC1** (Eq. 13c) for the vertical symmetric channel or **BC2** (Eqs. 13b-c) for the inclined isothermal asymmetrically wetted channel. The plates are maintained at a fixed temperature T_w = 20°C, which is supposed to be the liquid water film temperature. The boundary condition for the film is that of saturated air at T_w, hence ω_w = 14.5 g/kg. The Reynolds number is set at 300 and the channel's aspect ratio is γ = 1/65 for BC1 and γ = 1/50 for BC2.

4.1 Flow structure

Figure 3 presents the axial velocity profiles for the vertical symmetric channel. The case of forced convection ($Gr_M = Gr_T = 0$) is also reported to point out the effects of buoyancy forces. Close to the channel entrance (X = 0.15) the velocity profiles for mixed and forced convection are quite close, due to the prevalence of the viscous forces in the developing

boundary layer. As the air moves downstream, these forces become weak and the effect of buoyancy forces becomes clear. As both thermal and solutal Grashof numbers are negative, buoyancy forces act in the opposite direction of the upward flow and decelerate it near the walls. This deceleration produces a flow reversal close to the channel walls at *X = 2.31*. Buoyancy forces introduce a net distortion of the axial velocity profile compared to the case of forced convection. The flow reversal is clear in Figure 4, which show the evolution of the axial velocity, near the plates. Three different temperatures at the channel inlet are represented in this figure: T_0= 30°C (Gr_T= -0.88.10^5 and Gr_M=1.07.10^4), 41°C (Gr_T= -1.71.10^5 and Gr_M= 0) and 50°C (Gr_T= -2.29.10^5 and Gr_M=-1.29.10^4). We notice that the axial velocity takes negative values for the last two cases over large parts of the channel length. Along these intervals, air is flowing in the opposite direction of the entering flow. That change in the flow direction gives rise to a recirculation cell and to the flow reversal phenomenon.
Figure 5 shows the streamlines for the vertical symmetric channel. Two recirculation cells are present close to the channel entrance. Careful inspection of Fig. 5 show that the streamlines contours in the recirculation cells are open near the plates. Indeed, these streamlines are normal to the channel walls. Local velocity is then directed to these walls, as condensation occurs here (Oualid et al., 2010b).

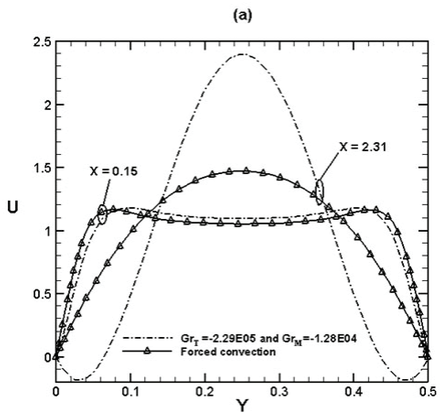

Fig. 3. Axial velocity profiles in the vertical symmetric channel for T_0= 50°C and ϕ_0 = 30% (Oulaid et al., 2010b)

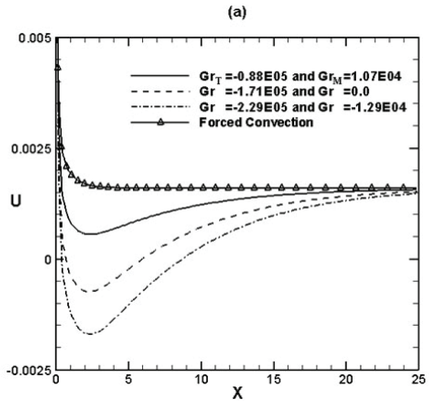

Fig. 4. Evolution of the axial velocity near the plates of the vertical symmetric channel for ϕ_0 = 30% at Y=1.33 10^{-4} (Oulaid et al., 2010b)

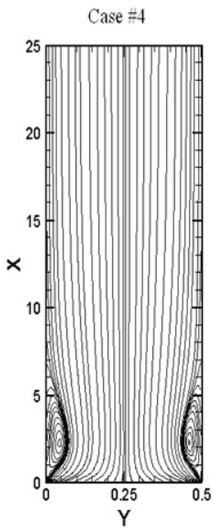

Fig. 5. Streamlines in the vertical symmetric channel for T_0= 41°C and ϕ_0 = 43.25% (Gr_T = -1.71.10^5 and Gr_M= -10^4) (Oulaid et al., 2010b).

For the inclined isothermal asymmetrically wetted channel, the flow structure is represented in Fig. 6 by the axial velocity profiles for different inclination angles. Remember that for this case only the lower plate (Y=0) is wet while the upper one is dry. The maximum of distortion of U is obtained for the vertical channel, for which buoyancy forces takes their maximum value in the axial direction. Fig. 6 show that flow reversal occurs for φ = 60° and

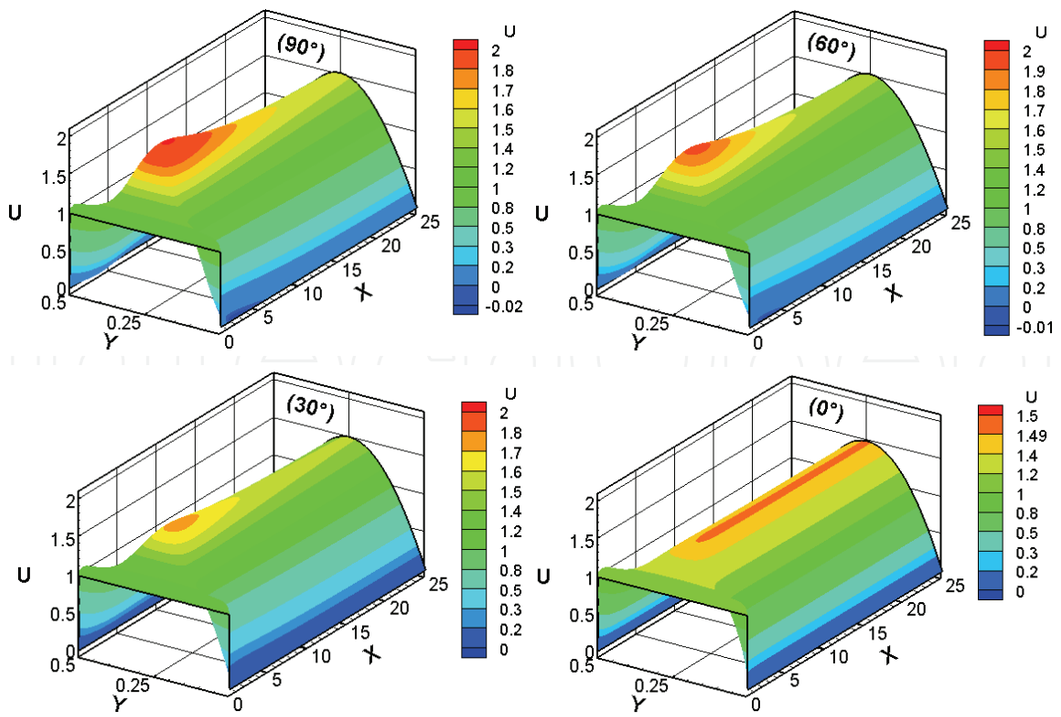

Fig. 6. Axial velocity profiles in the inclined isothermal asymmetrically wetted channel for T_0= 40°C and ϕ_0= 45.5% (Gr_T= -1.64 10^5 and Gr_M= -10^4) (Oulaid et al., 2010d).

90°. This is clearer from Fig. 9, which presents the friction factor *f* at the lower wet plate in the isothermal asymmetrically wetted channel. Negative values of *f* occur in the flow reversal region. Streamlines presented in Fig. 8, show the recirculation cells near the lower wet plate, where the airflow is decelerated due to its cooling. It can be seen clearly from Fig. 8 that the streamlines contours in the flow reversal region are not closed. Indeed, close to the lower wet plate, airflow velocity is directed towards the channel wall. This velocity, which is equal to the vapour velocity at the air-liquid interface V_e, is shown in Fig. 9. It is noted that V_e is negative which indicate that water vapour is transferred from airflow towards the wet plate. Thus, this situation corresponds to the condensation of the water vapour on that plate. It is interesting to note that close to the channel entrance, (X < 4.37) the magnitude of V_e for forced convection (and the horizontal channel too) is larger than for the inclined channel; while further downstream forced convection results in lower values of V_e magnitude. This inversion in V_e tendency occurs at the end of the flow reversal region (X = 4.37). In this region, as the channel approaches its vertical position, buoyancy forces slowdown airflow thus, water vapour condensation diminishes.

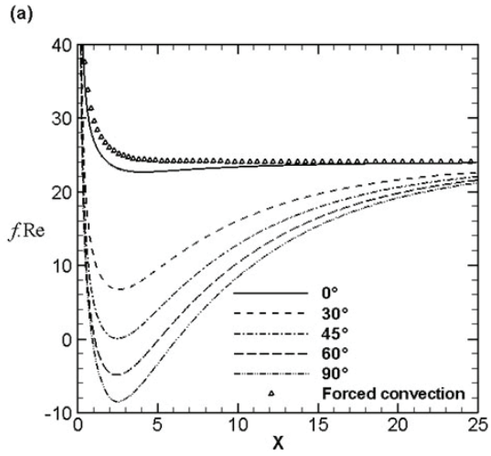

Fig. 7. Axial evolution of the friction factor at the lower wet plate in the isothermal asymmetrically wetted channel for T_0= 40°C and ϕ_0= 45.5% (Gr_T= -1.64 10^5 and Gr_M= -10^4) and different inclination angles (Oulaid et al., 2010d).

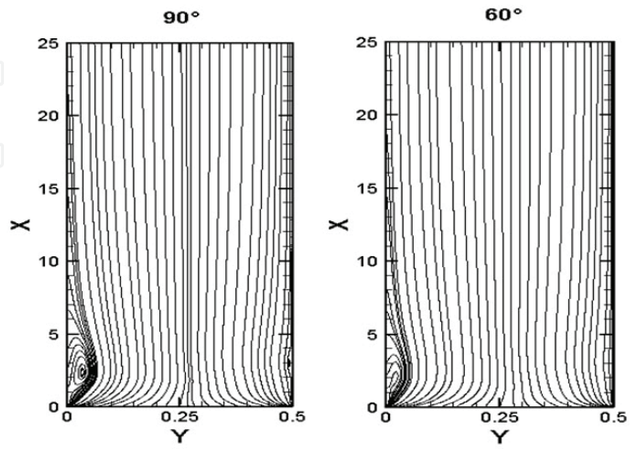

Fig. 8. Streamlines in the isothermal asymmetrically wetted channel for T_0= 40°C and ϕ_0= 45.5% (Gr_T= -1.64 10^5 and Gr_M= -10^4) and different inclination angles (Oulaid et al., 2010d).

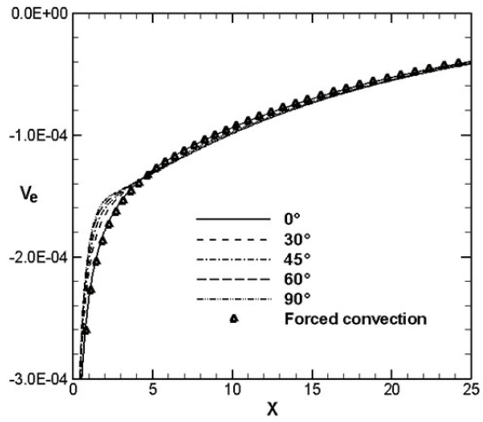

Fig. 9. Vapour velocity at the lower plate of the isothermal asymmetrically wetted channel for T_0= 40°C and ϕ_0= 45.5% (Gr_T= -1.64 10^5 and Gr_M= -10^4) and different inclination angles (Oulaid et al., 2010d).

4.2 Thermal and mass fraction characteristics

Figure 10 presents the evolution of the latent Nusselt number (Nu_L) at the wet plate of the isothermal asymmetrically wetted inclined channel. Nu_L is positive indicating that latent heat flux is directed towards the wet plate. Thus, water vapour contained in the air is condensed on that plate, as shown in Fig. 9. As the air moves downstream, water vapour is removed from the air; thus, the gradient of mass fraction decreases, and that explains the decrease in Nu_L. In the first half of the channel, Nu_L is less significant as the channel approaches its vertical position, due to the deceleration of the flow by the opposing buoyancy forces as depicted above. Close to the channel exit, the buoyancy forces magnitude diminishes; hence, Nu_L takes relatively greater values for the vertical channel (Oulaid et al., 2010a). Figure 11 show the Sensible Nusselt number at the wet plate of the isothermal asymmetrically wetted channel. It is clear that the buoyancy forces diminish heat transfer. This diminution is larger in the recirculation zone. Figure 12 presents Sherwood number at the wet plate of the isothermal asymmetrically wetted channel. The behaviour of Sh resembles to that of Nu_S, as Le ≈ 1 here.

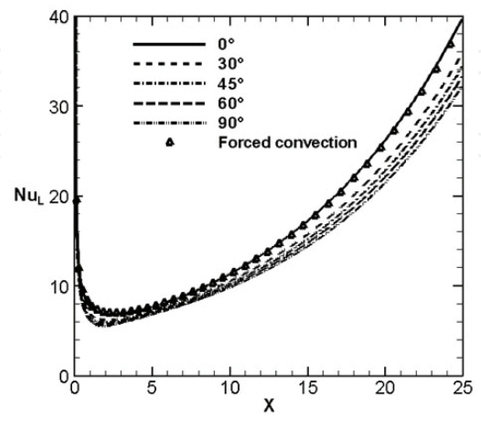

Fig. 10. Latent Nusselt number at the wet plate of the isothermal asymmetrically wetted inclined channel for T_0= 40°C and ϕ_0= 45.5% (Gr_T= -1.64 10^5 and Gr_M= -10^4) and different inclination angles (Oulaid et al., 2010d).

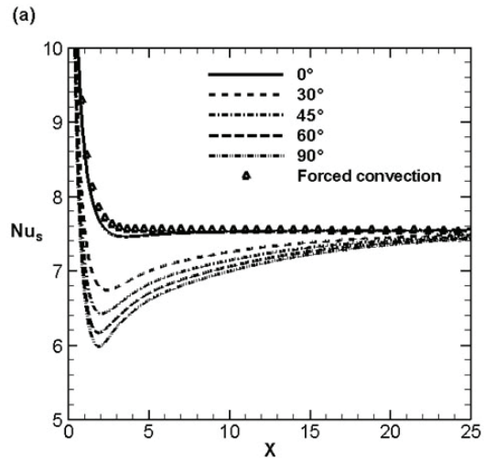

Fig. 11. Sensible Nusselt number Nu_S at the wet plate of the isothermal asymmetrically wetted inclined channel for T_0= 40°C and ϕ_0= 45.5% (Gr_T= -1.64 10^5 and Gr_M= -10^4) and different inclination angles (Oulaid et al., 2010d).

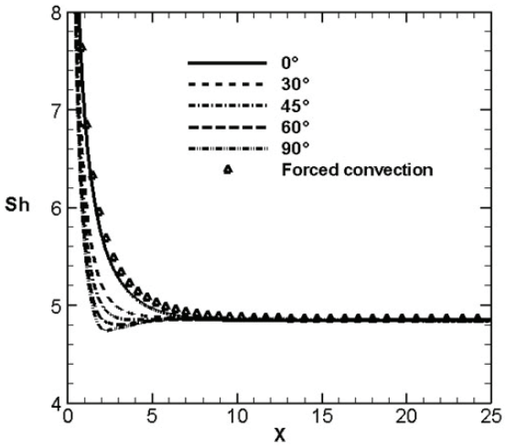

Fig. 12. Sherwood number Sh at the wet plate of the isothermal asymmetrically wetted inclined channel for T_0= 40°C and ϕ_0= 45.5% (Gr_T= -1.64 10^5 and Gr_M= -10^4) and different inclination angles (Oulaid et al., 2010d).

4.3 Flow reversal chart

As stated in the introduction, flow reversal in heat-mass transfer problems was not studied extensively in the literature. This phenomenon is an important facet of the hydrodynamics of a fluid flow and its presence indicates increased flow irreversibility and may lead to the onset of turbulence at low Reynolds number. Hanratty et al. (1958) and Scheele & Hanratty (1962) were pioneers in experimental study of flow reversal in vertical tube mixed convection. These authors have shown that the non-isothermal flow appears to be highly unstable and may undergo its transition from a steady laminar state to an unstable one at rather low Reynolds number. The unstable flow structure has shown, the 'new equilibrium' state that consisted of large scale, regular and periodic fluid motions. The condition of the existence of flow reversal in thermal mixed convection flows were established by many authors for different conditions (Wang et al. 1994; Nesreddine et al. 1998, Zghal et al. 2001;

Behzadmehr et al. 2003). As heat and mass transfer mixed convection is concerned, such studies are rare as depicted in the introduction.

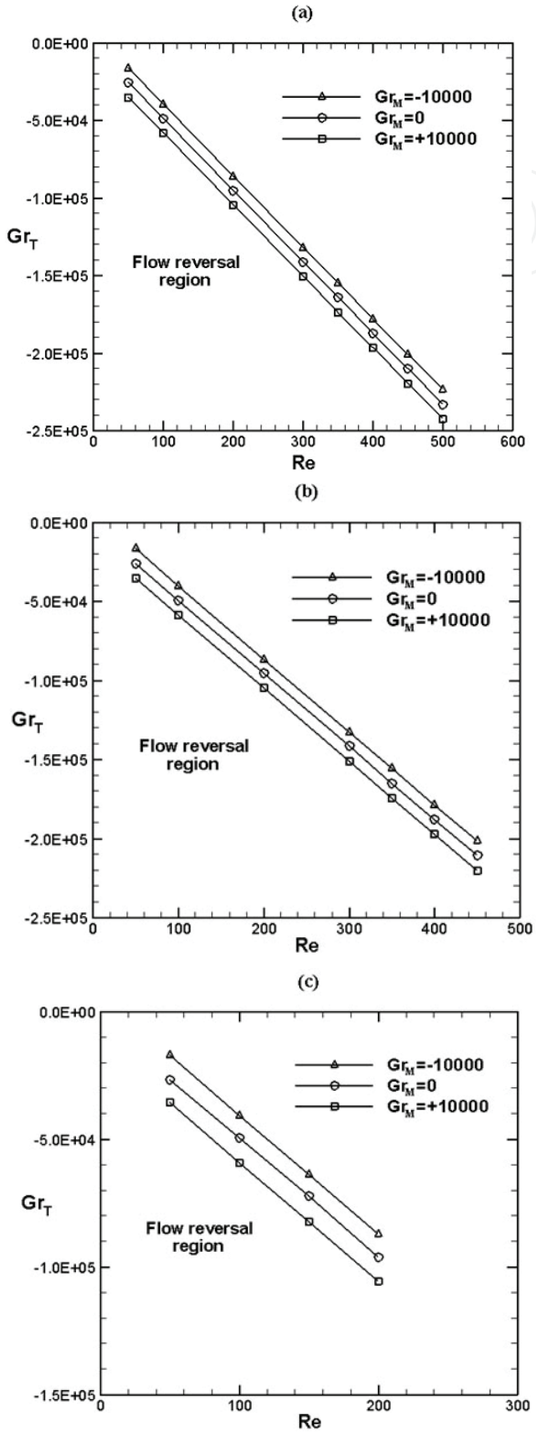

Fig. 13. Flow reversal chart for the vertical symmetric channel (a) $\gamma = 1/35$, (b) $\gamma = 1/50$ and (c) $\gamma = 1/65$. (Oulaid et al. 2010b)

The conditions for the existence of flow reversal was established in the symmetric vertical channel (Oulaid et al., 2010b) and the isothermal asymmetrically wetted inclined channel (Oulaid et al., 2010d). For a given Re we varied T_0 (i.e. Gr_T) at fixed Gr_M (i.e. ϕ_0) in asequence of numerical experiments until detecting a negative axial velocity. All the considered combinations of temperature and mass fraction satisfy the condition for the application of the Oberbeck-Boussinesq approximation, as the density variations do not exceed 10%. These series of numerical experiments enabled us to draw the flow reversal charts for different aspect ratios of the channel (γ = 1/35, 1/50 and 1/65). These flow reversal charts are presented in Figs 13-14. These charts would be helpful to avoid the situation of unstable flow associated with flow reversal. The flow reversal charts are also expected to fix the validity limits of the mathematical parabolic models frequently used in the heat-mass transfer literature (Lin et al., 1988; Yan et al., 1991; Yan and Lin, 1991; Debbissi et al., 2001; Yan, 1993; Yan et al., 1990; Yan and Lin, 1989; Yan, 1995).

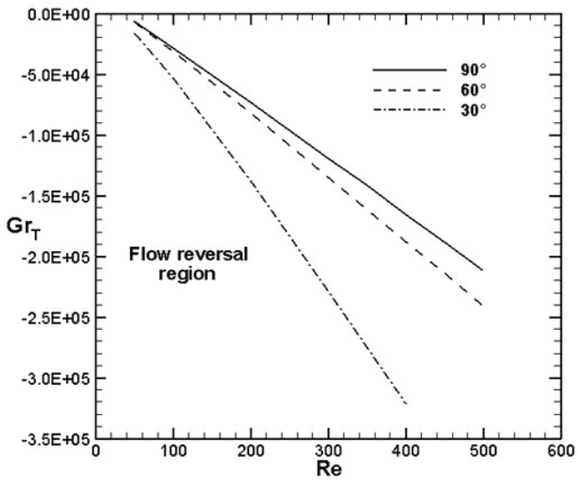

Fig. 14. Flow reversal chart in the isothermal asymmetrically wetted inclined channel for $Gr_M = -10^4$ and $\gamma = 1/65$ (Oulaid et al. 2010d)

5. Asymmetrically cooled channel

For the asymmetrically cooled parallel-plate channel, the plates are subject to the boundary condition **BC3** (i.e. one of the plates is wet and maintained at a fixed temperature T_w = 20°C, while the other is dry and thermally insulated). The Reynolds number is set at 300 and the channel's aspect ratio is γ = 1/130 (L =2m).

5.1 Flow structure

The streamlines for the asymmetrically cooled vertical channel is presented in Fig. 15. This figure shows the recirculation cell, which is induced by buoyancy forces. The dimension of this recirculation cell is more significant than in the case of the isothermal channel (Figs. 5 and 8). The recirculation cell occupies a larger part of the channel and its eye is closer to the channel axis. The flow structure is strongly affected by the buoyancy forces. These forces induce a momentum transfer from the wet plate, where the flow is decelerated, towards the dry plate, where the flow is accelerated (Kassim et al. 2010a).

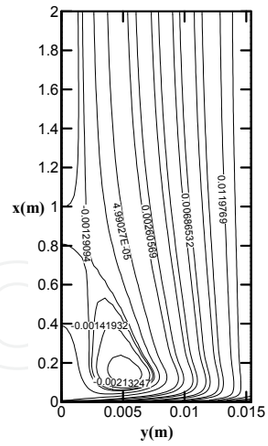

Fig. 15. Streamlines in asymmetrically cooled vertical channel for T_0 =70°C and ϕ_0 = 70% (Gr_T= - 1′208′840 and Gr_M= -670′789) (Kassim et al. 2010a)

5.2 Thermal and mass fraction characteristics

The vapour mass flux at the liquid-air interface is shown in Figure 16. The represented cases correspond to vapour condensation (water vapour contained in airflow is condensed at the isothermal wetted plate in all cases). For ϕ_0 = 10%, phase change and mass transfer at the liquid-air interface is weak, thus condensed mass flux decreases rapidly and stretches to zero. Considering the other cases (ϕ_0 = 30% or 70%) the behaviour of the condensed mass flux is complex. It exhibits local extrema, which are more pronounced as ϕ_0 is increased. Its local minimum occurs at the same axial location of the recirculation cell eye (Fig. 15). Thus, it can be deduced that the increase of the vapour mass flux towards its local maximum is attributed to the recirculation cell. The latter induces a fluid mixing near the isothermal plate and thus increases condensed mass flux. As the recirculation cell switches off, the condensed mass flux decreases due to the boundary layer development.

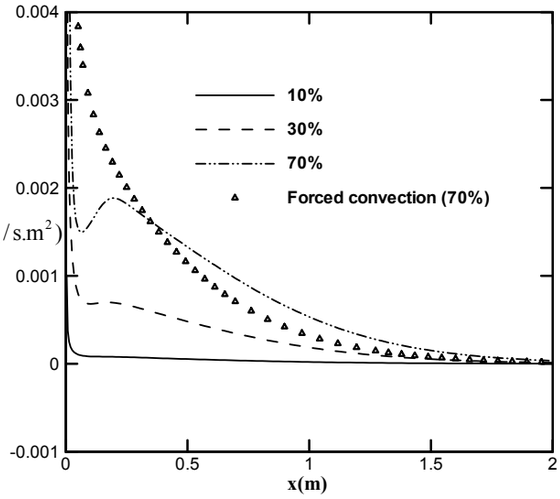

Fig. 16. Vapour mass flux at the wet plate in asymmetrically cooled vertical channel of T_0= 70°C and different inlet humidity ϕ_0= 10% (Gr_T= - 1′180′887 and Gr_M= - 24′359), 30% (Gr_T= - 1′189′782 and Gr_M= - 226′095) and 70% (Gr_T= - 1′208′840 and Gr_M= - 670′789) (Kassim et al. 2010a)

Figure 17 presents axial development of airflow temperature at the channel mid-plane (y= 0.0068m). Airflow is being cooled in all cases as it goes downstream, due to a sensible heat transfer from hot air towards the isothermally cooled plate. The airflow temperature at the channel mid-plane exhibits two local extremums near the channel entrance. These extremums are more pronounced for ϕ_0 = 70%. In this case the local minimum of air temperature is 44.24°C which occurs at x = 0.092m and the local maximum is 46.59°C which occurs at x = 0.208m. These axial locations are closer to that corresponding to local minimum and maximum of the condensed mass flux (Fig. 16). Once again, it is clear that the existenceof local extremums of air temperature at the channel mid-plane is related to the fluid mixing induced by flow reversal near the isothermal wet plate. This fluid mixing increases the condensed mass flux, thus the airflow temperature increases. Indeed, vapour condensation releases latent heat, which is partly absorbed by airflow. Moreover, close to the channel inlet, airflow at the channel mid-plane is cooler as ϕ_0 is increased. In this region the buoyancy forces decelerate the upward airflow and induce flow reversal and thus, increase the air-cooling through sensible heat transfer towards the isothermal plate (Kassim et al. 2010a).

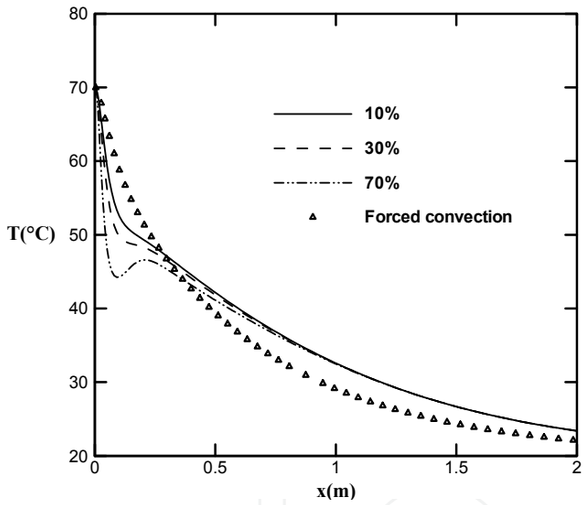

Fig. 17. Airflow temperature at the mid-plane (y = 0.0074m) of the asymmetrically cooled vertical channel for T_0= 70°C and different inlet humidity ϕ_0= 10% (Gr_T= - 1'180'887; Gr_M= - 24'359), 30% (Gr_T= - 1'189'782; Gr_M= - 226'095) and 70% (Gr_T= - 1'208'840; Gr_M= - 670'789) (Kassim et al. 2010a)

Axial evolution of the local latent Nusselt number Nu_L at the isothermal plate is represented in Fig. 18. For ϕ_0 = 10%, Nu_L diminishes and stretches to zero at the channel exit, as phase change and mass transfer at the liquid-air interface is weak (Fig. 16). The axial evolution of Nu_L for ϕ_0 = 30% and 70%, is more complex and exhibits local minimum and maximum. The positions of these extremums, which are the same as for the vapour mass flo rate at the liquid-air interface (Fig. 16), depend on ϕ_0 and are more pronounced for ϕ_0 = 70%. Furthermore, the development of Nu_L and $\dot{m}$ is analogous. Thus, the occurrence of the local extremums of Nu_L is due to the interaction between the vapour condensation and flow reversal as explained above.

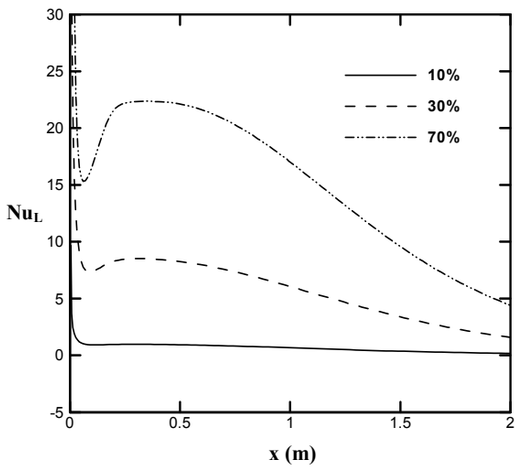

Fig. 18. Latent Nusselt number at the wet plate of the asymmetrically cooled vertical channel for T_0= 70°C and different inlet humidity ϕ_0= 10% (Gr_T= - 1′180′887; Gr_M= - 24′359), 30% (Gr_T= - 1′189′782; Gr_M= - 226′095) and 70% (Gr_T= - 1′208′840; Gr_M= - 670′789) (Kassim et al. 2010a)

6. Insulated walls

The channel walls are subject to the boundary condition **BC4** (i.e., both of the plates are thermally insulated and wet). In this case, an experimental study was conducted and its resuts are compared to the numerical one. Detailed description of the experimental setup is given by Cherif et al. (2010). Only some important aspects of this setup are reported here. The channel is made of two square stainless steel parallel plates (50cm by 50cm) and two Plexiglas rectangular parallel plates (50cm by 5cm). Thus, the channel's aspect ratio is γ = 1/10. The channel is vertical and its steel plates are covered on their internal faces with falling liquid films. In order to avoid dry zones and wet the plates uniformly, very thin tissues support these films. Ambient air is heated through electric resistances and upwards the channel, blown by a centrifugal fan, via an settling box equipped with a honeycomb. Airflow and water film temperature are measured by means of Chromel-Alumel (K-type) thermocouples. For the liquid films, ten thermocouples are welded along each of the wetted plates. For the airflow, six thermocouples are placed on a rod perpendicular to the channel walls. This rod may be moved vertically in order to obtain the temperature at different locations. The liquid flow rate is low and a simple method of weighing is sufficient to measure it. The evaporated mass flux was obtained by the difference between the liquid flow rate with and without evaporation (Cherif et al, 2010; Kassim et al. 2009; Kassim et al. 2010b). The liquid film flow rate was set between 1.55 10^{-4} $kg.s^{-1}.m^{-1}$ and 19.4 10^{-4} $kg.s^{-1}.m^{-1}$. These values are very low compared to the considered mass fluxes in Yan (1992; 1993). Thus, it is expected that the *zero film thickness model* will be valid. The comparison of the numerical and experimental results is conducted for laminar airflow. The Reynolds number is set at 1620 (U_0 = 0.27 m/s).

The airflow temperature is presented in Fig. 19 at three different axial locations. It is clear that the concordance between the experimental measurements and the numerical results is satisfactory. This concordance is excellent at the plates and close to it. Nevertheless, the difference between these results does not exceed 8% elsewhere. It is noted that airflow is

cooled as it upwards the channel. This cooling essentially occurs in the vicinity of the wet plates. The wet plates temperature profile is presented in Fig. 20. It should be noted that, in the experimental study, T_w is the water film temperature. The comparison between the measurements and the numerical results is good, as the difference is less than 1.5%. It can be deduced that the assumption of extremely thin liquid film, adopted in the numerical model, is reliable here. On the other hand, it is noted that the liquid film is slightly cooled and then a bit heated in contact with the hot airflow. It is important to remind that air enters the channel at x=0m while the water film enters at x=0.5m. However, the water film temperature remains quasi-constant within 2.5°C. It can be deduced that air is cooled mostly by latent heat transfer associated to water evaporation. The global evaporated mass flux is presented in Fig. 21 with respect to the inlet air temperature T_0. This mass flux is calculated in the numerical study by the following equation,

$$\dot{m}_{ev} = \frac{1}{L}\int_0^L \rho V_e \, dx \tag{25}$$

Experimentations were performed for three inlet air temperature 30, 35 et 45°C. Fig. 21 shows that the evaporated mass flux increases as the inlet air temperature is increased. This is attributed to the increase of sensible heat transfer from the airflow to the water film, which results in mass transfer from the film to the airflow associated with water evaporation. Meticulous examination of Fig. 21 reveals that numerical calculation predicts well the measured evaporated mass flux for T_0 = 30°C. For larger inlet air temperature, the mathematical model underestimates the evaporated mass flux. Indeed the discrepancy between the calculations and the measurements increases with T_0. It is believed that this is due to the calculation method. Indeed, in Eq 25 the density is considered constant and calculated at the reference temperature (obtained by the *one third rule*). However, global agreement between the calculations and the measurements is found in Fig. 21 as the discrepancy does not exceed 10%.

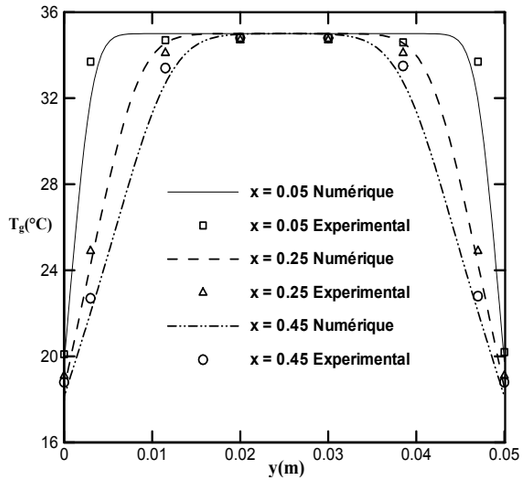

Fig. 19. Airflow temperature profiles at different axial locations for the insulated parallel-plate vertical channel (Kassim et al., 2010b). *Experimental conditions: u_0 = 0.27m/s, Re = 1620, water flow rate =1.5 l/h, inlet liquid temperature= 17.7°C, ambient air humidity = 41% and temperature = 18.2 °C, inlet airflow humidity ϕ_0 = 16% and temperature T_0 = 45°C.*

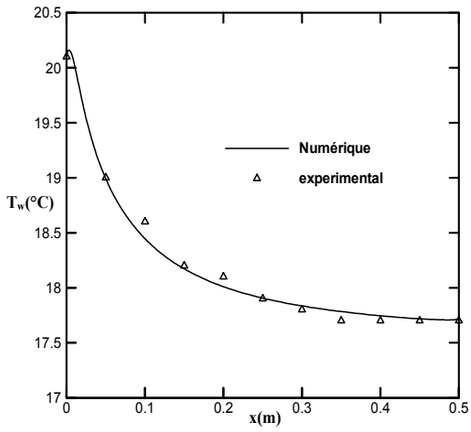

Fig. 20. Wall temperature for the insulated parallel-plate vertical channel (Kassim et al., 2009). Experimental conditions: u_0 = 0.27m/s, Re = 1620, water flow rate = l/h, inlet liquid temperature= 18°C, ambient air humidity = 45% and temperature = 19 °C, inlet airflow humidity ϕ_0 = 16 and temperature T_0 = 45°C.

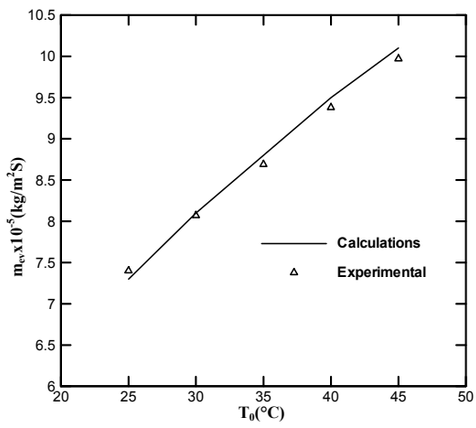

Fig. 21. Evaporated mass flux at the liquid-air interface (Kassim et al., 2009). Experimental conditions: u_0 = 0.27m/s, Re = 1620, water flow rate =1 l/h, inlet liquid temperature= 18°C, ambient air humidity = 45% and temperature = 19 °C.

7. Conclusion

Heat and mass transfer mixed convection in channels, with special emphasis on phase change and flow reversal, is considered. The literature review reveals that the flow reversal phenomenon in such problems was not extensively studied. Some recent numerical and experimental work of the authors are reported. The chanel is a parallel-plate one, which may be isothermally cooled or thermally insulated. Water liquid films stream along one or both of the plates. The effects of buoyancy forces on the flow structure as well as on heat and mass transfer characteristics are analysed. The conditions of the occurrence of flow reversal are particularly addressed. Flow reversal charts, which specify these conditions, are given. The comparison between the numerical and experimental results is satisfactory. However,

the numerical study is limited by its hypotheses. Future research may concern more elaborated mathematical models taking into account the variability of the thermo-physical properties and the thickness of the liquid film. On the other hand, as flow reversal may induce flow instability, a transient mathematical model, such as the low Reynolds number turbulence model may be more appropriate. Finally, more experimental investigations of the considered problem is needed.

8. Acknowledgements

The experimental study was conducted at the *Laboratoire d'Energétique et des Transferts Thermiques et Massiques, Faculty of Sciences, Bizerte* (Tunisa) . The financial support of the Morocco-Tunisian Cooperation Program (Grant no MT/06/41) is acknowledged.

9. Nomenclature

b	half width of the channel (m)
C	dimensionless mass fraction, = $(\omega - \omega_0) . (\omega_w - \omega_0)^{-1}$
D	mass diffusion coefficient [$m^2.s^{-1}$]
D_h	hydraulic diameter, = 4b [m]
f	friction factor
g	gravitational acceleration [$m.s^{-2}$]
Gr_M	mass diffusion Grashof number, = $g.\beta^*.D_h^3.(\omega_w - \omega_0).\nu^{-2}$
Gr_T	thermal Grashof number, = $g.\beta.D_h^3.(T_w - T_0).\nu^{-2}$
h	local heat transfer coefficient [$W.m^{-2}.K^{-1}$]
h_m	local mass transfer coefficient [$m.s^{-1}$]
h_{fg}	latent heat of vaporization [$J.kg^{-1}$]
k	thermal conductivity [$W\ m^{-1}\ K^{-1}$]
L	channel height [m]
$\dot{m}$	vapour mass flux at the liquid-gas interface [$kg.s^{-1}.m^{-2}$]
M_a	molecular mass of air [$kg.kmol^{-1}$]
M_v	molecular mass of water vapour [$kg.kmol^{-1}$]
N	buoyancy ratio, = Gr_M/Gr_T
Nu_S	local Nusselt number for sensible heat transfer
Nu_L	local Nusselt number for latent heat transfer
p	pressure
P_m	modified dimensionless pressure, = $(p + \rho_0\ g\ x).(\rho_0\ u_0^2)^{-1}$
Pr	Prandtl number, = ν/α
q"	heat flux [$W.m^{-2}$]
Re	Reynolds number, = $u_0.D_h.\nu^{-1}$
R_{Nu}	ratio of latent to sensible Nusselt numbers, = Nu_L/Nu_S
Sc	Schmidt number, = ν/D
Sh	Sherwood number
T	temperature [K]
u, v	velocity components [$m.s^{-1}$]
U, V	dimensionless velocity components, = u/u_0, v/u_0
V_e	dimensionless transverse vapour velocity at the air-liquid interface.

x, y axial and transverse co-ordinates [m]
X, Y dimensionless axial and transverse co-ordinates, = x/D_h, y/D_h

Greek symbols

α thermal diffusivity [$m^2\ s^{-1}$]
β coefficient of thermal expansion,
β^* coefficient of mass fraction expansion,
γ aspect ratio of the channel, = 2b/L
Θ dimensionless temperature, = $(T - T_0)/(T_w - T_0)$
ν kinematic viscosity [$m^2.s^{-1}$]
ρ density [$kg.m^{-3}$]
ϕ relative humidity (%)
φ inclination angle of the channel
ω mass fraction [kg of vapour/ kg of mixture]

Subscripts

a relative to the gas phase (air)
L relative to latent heat transfer
ℓ relative to the liquid phase
m mean value
0 at the inlet
S relative to sensible heat transfer
sat at saturation conditions
v relative to the vapour phase
w at the wall

10. References

Agunaoun A., A. Daif, R. Barriol, & M. Daguenet (1994), Evaporation en convection forcée d'un film mince s´écoulant en régime permanent, laminaire et sans ondes, sur une surface plane inclinée, *Int. J. Heat Mass Transfer*, 37, 2947–2956.

Agunaoun A., A. IL Idrissi, A. Daıf, & R. Barriol (1998) Etude de l'évaporation en convection mixte d'un film liquide d'un mélange binaire s'écoulant sur une plaque inclinée soumise à un flux de chaleur constant, *Int. J. Heat Mass Transfer*, 41, 2197–2210.

Ait Hammou Z., B. Benhamou, N. Galanis & J. Orfi (2004), Laminar mixed convection of humid air in a vertical channel with evaporation or condensation at the wall, *Int. J. Thermal Sciences*, 43, 531-539.

Azizi Y., B. Benhamou, N. Galanis & M. El Ganaoui (2007), Buoyancy effects on upward and downward laminar mixed convection heat and mass transfer in a vertical channel», *Int. J. Num. Meth. Heat Fluid Flow*, 17, 333-353.

Baumann W.W. & Thiele F., (1990) Heat and mass transfer in evaporating two-component liquid film flow, *Int. J. Heat Mass Transfer*, 33, 273–367.

Behzadmehr A., Galanis N., Laneville A., (2003) Low Reynolds number mixed convection in vertical tubes with uniform wall heat flux, Int. J. Heat Mass Transfer 46, 4823–4835.

Ben Nasrallah S. & Arnaud G. (1985) Évaporation en convection naturelle sur une plaque verticale chauffée à flux variable. *Journal of Applied Mathematics and Physics*, 36, 105-119.

Boulama, K., Galanis, N., (2004) Analytical solution for fully developed mixed convection between parallel vertical plates with heat and mass transfer, *J. Heat Transfer*, 126, 381–388.

Burmeister, L.C., (1993) *Convective Heat Transfer*, J. Wiley, New York.

Chang C. J., Lin T. F. & Yan W. M., (1986) Natural convection flows in a vertical open tube resulting from combined buoyancy effects of thermal and mass diffusion, *Int. J. Heat Mass Transfer,* 29, 1453-1552.

Chow, L.C., & Chung, J.N. (1983), Evaporation of water into laminar stream of air and superheated steam, *Int. J. Heat Mass Transfer*, 26, 373-380.

A. S. Cherif, M. A. Kassim, B. Benhamou, S. Ben Jabrallah, S. Harmand, J.P. Courriou "Experimental Study of Mixed Convection Heat and Mass Transfer in a Vertical Channel with Film Evaporation", *Int. Journal Thermal Science*, Submitted June 2010.

Fedorov A. G., R. Viskanta & A. A. Mohamad (1997) Turbulent heat and mass transfer in assymetrically heated, vertical parallel plate channel, *Int. J. Heat and Fluid Flow*, 18, 307–315.

Feddaoui M., Mir A. & Belahmidi E. (2003) Cocurrent turbulent mixed convection heat and mass transfer in falling film of water inside a vertical heated tube, *Int. J. Heat Mass Transfer*, 46, 3497–3509.

Fuji, T., Kato, Y. & Bihara, K. (1977), *Expressions of transport and thermodynamic properties of air, steam and water*, Sei San Ka Gaku Ken Kuu Jo, Report no 66, Kyu Shu University, Kyu Shu, Japan.

Gebhart B. & Pera L. (1971), The nature of vertical natural convection flows resulting from the combined buoyancy effects of thermal and mass diffusion, *Int. J. Heat Mass Transfer*, 14, 2025-2050.

Gebhart B., Jaluria Y., Mahajan R. L. & Sammakia B. (1988), *Buoyancy-induced flows and transport*, Hemisphere Pub. Co., New York.

Hanratty T. J., Rosen E. M., Kabel R. L. (1958), Effect of heat transfer on flow field at low Reynolds numbers in vertical tubes, *Indust. Engrg. Chem.*, 50, 815-820.

He S., An P., Li J. & Jackson J.D. (1998) Combined heat and mass transfer in a uniformly heated vertical tube with water film cooling, *Int. J. Heat Fluid Flow*, 19, 401-417.

Hubbard G.L., Denny, V.E. & Mills, A.F. (1975), Droplet evaporation: effects of transients and variable properties, *Int. J. Heat Mass Transfer*, 18, 1003-1008.

Huang, C.C. Yan, W.M. and Jang, J.H. (2005), Laminar mixed convection heat and mass transfer in a vertical rectangular duct with film evaporation and condensation, *Int. J. Heat Mass Transfer*, 48, 1772-1784.

Kassim M. A., Benhamou B. & Harmand S. (2010a) Combined heat and mass transfer with phase change in a vertical channel, *Computational Thermal Science*, 2, 299-310.

Kassim M. A., Cherif A. S., Benhamou B., Harmand S. et Ben Jabrallah S. (2010b) étude numérique et expérimentale de la convection mixte thermosolutale accompagnant un écoulement d'air laminaire ascendant dans un canal vertical adiabatique. *1*er *Colloque International Francophone d'Energétique et Mécanique (CIFEM'2010),* Saly, 17-19 mai 2010, Senegal.

Kassim M. A., Benhamou B., Harmand S., Cherif A. S., Ben Jabrallah S. (2009) " Etude numérique et expérimentale sur les transferts couplés de chaleur et de masse avec changement de phase dans un canal vertical adiabatique " IXème Colloque Inter-universitaire Franco–Québécois Thermique des systèmes CIFQ2009, 18-20 mai 2009, Lille, France

Laaroussi N., Lauriat G. & Desrayaud G. (2009), Effects of variable density for film evaporation on laminar mixed convection in a vertical channel, *Int. J. Heat Mass Transfer*, 52, 151-164.

Lin T.F., Chang C.J., & Yan W.M. (1988), Analysis of combined buoyancy effects of thermal and mass diffusion on laminar forced convection heat transfer in a vertical tube, *ASME J. Heat Transfer* 110, 337–344.

Lin, J. N., Tzeng, P. Y., Chou, F. C., Yan, W. M. (1992), Convective instability of heat and mass transfer for laminar forced convection in the thermal entrance region of horizontal rectangular channels, *Int. J. Heat Fluid Flow*, 13, 250-258.

Maurya R. S., Diwakar S. V., Sundararajan T., & Das Sarit K. (2010), Numerical investigation of evaporation in the developing region of laminar falling film flow under constant wall heat flux conditions, Numerical Heat Transfer, Part A, 58: 41–64

Maré, T., Galanis, N., Voicu, I., Miriel, J., Sow, O., (2008) Experimental and numerical study of mixed convection with flow reversal in coaxial double-duct heat exchangers, *Exp. Therm. Fluid Sci.*, 32, 1096–1104.

Mezaache H. & Daguenet M. (2000) Etude numérique de l'évaporation dans un courant d'air humide laminaire d'un film d'eau ruisselant sur une plaque inclinée, *Int. J. Thermal Sci.*, 39, 117–129.

Minkowycz, W.J. & Sparrow E.M. (1966), Condensation heat transfer in the presence of non-condensable, interfacial resistance, superheating, variable properties, and diffusion, *Int. J. Heat Mass Transfer,* 9, 1125–1144

Nesreddine, H., Galanis, N. & Nguyen, C.T., (1998) Effects of axial diffusion on laminar heat transfer with low Péclet numbers in the entrance region of thin vertical tubes. Numer. Heat Transfer Part A, 33, 247–266.

Nelson D. J. & Wood B. D. (1989) Combined heat and mass transfer natural convection between vertical parallel plates, Int. J. Heat Mass Transfer, 328, 1779–1789.

Nguyen, C.T., Maiga, S.E., Landry, M., Galanis, N., Roy, G. (2004) Numerical investigation of flow reversal and instability in mixed laminar vertical tube flow, *Int. J. Therm. Sci.*, 43, 797–808.

Nusselt, W. (1916) Die Oberflchenkondensation des Wasserdampfes, *Z. Ver. Deutch. Ing.* 60 541–546. 569–575.

Oulaid O., B. Benhamou, N. Galanis (2010a), Combined buoyancy effects of thermal and mass diffusion on laminar forced convection in a vertical isothermal channel, *Computational Thermal Science*, 2, 125-138.

Oulaid O., Benhamou B., Galanis N. (2010b), Mixed Convection Heat and Mass Transfer with Phase Change and Flow Reversal in Channels, *Int. J. Heat Fluid Flow*, 31, 711-721 (*doi:10.1016/j.ijheatfluidflow.2010.04.007*).

Oulaid O., Benhamou B., Galanis N. (2010c), Simultaneous heat and mass transfer in inclined channel with asymmetric conditions, *14th Int. Heat Transfer Conference IHTC14,* Washigton USA, 8-13 August 2010

Oulaid O., Benhamou B., Galanis N. (2010d), Simultaneous heat and mass transfer in inclined channel with asymmetric conditions, *Journal of Applied Fluid Mechanics*, *in press*.

Oulaid Othmane (2010), *Transferts couplés de chaleur et de masse par convection mixte avec changement de phase dans un canal*, Ph. D. Thesis, Jointly presented at Cadi Ayyad Univesity Marrakech (Morocco) and University of Sherbrooke (Canada).

Oulaid O., B. Benhamou, N. Galanis (2009), "Effet de l'inclinaison sur les transferts couplés de chaleur et de masse dans un canal" *IXème Colloque Inter-Universitaire Franco–Québécois Thermique des systèmes CIFQ2009*, 18-20 mai 2009, Lille, France

Oulaid O., B. Benhamou (2007), Effets du rapport de forme sur les transferts couples de chaleur et de masse dans un canal vertical, *Actes des 13èmes Journées Internationales de Thermique - JITH07*, pp. 76-80, Albi, France, 28-30 Aout 2007. (http://hal.archives-ouvertes.fr/docs/00/22/66/58/PDF/A20.pdf)

Patankar, S. V. (1980), *Numerical Heat Transfer and Fluid Flow*, Hemisphere/McGraw-Hill.

Patankar, S. V. (1981), A calculation procedure for two-dimensional elliptic situations, *Numerical Heat Transfer*, 4, 409-425.

Salah El-Din, M.M., (1992) Fully developed forced convection in vertical channel with combined buoyancy forces, *Int. Comm. Heat Mass Transfer,* 19, 239–248.

Scheele G. F., Hanratty T. J. (1962), Effect of natural convection on stability of flow in a vertical pipe, J. Fluid Mech., 14, 244-256.

Siow, E. C., Ormiston, S. J., Soliman, H. M. (2007), Two-phase modelling of laminar film condensation from vapour-gas mixtures in declining parallel-plate channels, *Int. J. Thermal Sciences*, 46, 458-466.

Suzuki K., Y. Hagiwara & T. Sato (1983), Heat transfer and flow characteristics of two-component annular flow, *Int. J. Heat Mass Transfer*, 26, 597-605.

Shembharkar T. R. & Pai B. R., (1986) Prediction of film cooling with a liquid coolant, *Int. J. Heat Mass Transfer*, 29, 899-908.

Tsay Y. L., Li T. F. et Yan W. M. (1990) Cooling of falling liquid film through interfacial heat and mass transfer. *Int. J. Multiphase Flow,* 16, 853-865.

Vachon M. (1979) Étude de l'évaporation en convection naturelle. *Thèse de Doctorat*, Université de Poitiers, Poitiers, France.

Volchkov E. P., Terekhov V. V., Terekhov V. I. (2004), A numerical study of boundary layer heat and mass transfer in a forced convection of humid air with surface steam condensation, *Int. J. Heat Mass Transfer*, 47, 1473-1481.

Wang, M., Tsuji, T., Nagano, Y., (1994) Mixed convection with flow reversal in the thermal entrance region of horizontal and vertical pipes, *Int. J. Heat Mass Transfer*, 37, 2305–2319. 656

Yan W.M., Y.L. Tsay & T.F. Lin (1989), Simultaneous heat and mass transfer in laminar mixed convection flows between vertical parallel plate with asymmetric heating, *Int. J. Heat Fluid Flow* 10, 262–269.

Yan W.M. & Lin T.F. (1989), Effects of wetted wall on laminar mixed convection heat transfer in a vertical channel, J. Thermophys. Heat Transfer, 3, 94–96.

Yan W. M., Y. L. Tsay & T. F. Lin (1990), Effects of wetted walls on laminar natural convection between vertical parallel plate with asymmetric heating, *Applied Scientific Research*, 47, 45-64.

Yan W.M. (1991), Mixed convection heat transfer enhancement through latent heat transport in vertical parallel plate channel flows, *Can J. Chem. Eng*., 69, 1277–1282.

Yan W. M., T. F. Lin & Y. L. Tsay (1991), Evaporative cooling of liquid film through interfacial heat and mass transfer in a vertical channel - I. Experimental study, *Int. J. Heat Mass Transfer*, 34, 1105-1111.

Yan W. M. & Lin T. F. (1991), Evaporative cooling of liquid film through interfacial heat and mass transfer in a vertical channel - II. Numerical study, *Int. J. Heat Mass Transfer* 34, 1113-1124.

Yan W. M. (1992), Effect of film evaporation laminar mixed convection heat and mass transfer in a vertical channel, *Int. J. Heat Mass Transfer,* 35, 3419–3429.

Yan, W.M. (1993), Mixed convection heat transfer in a vertical channel with film evaporation, *Canadian J. Chemical Engineering*, 71, 54-62.

Yan W.M. (1995a), Turbulent mixed convection heat and mass transfer in a wetted channel, *ASME J. Heat Transfer* 117, 229–233.

Yan W. M. (1995b), Effects of film vaporization on turbulent mixed convection heat and mass transfer in a vertical channel, *Int. J. Heat Mass Transfer*, 38, 713-722.

Yan W. M. & Soong C. Y. (1995) Convective heat and mass transfer along an inclined heated plate with film evaporation, Int. J. Heat Mass Transfer, 38, 1261-1269.

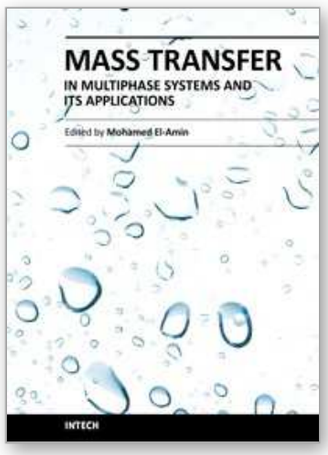

Mass Transfer in Multiphase Systems and its Applications
Edited by Prof. Mohamed El-Amin

ISBN 978-953-307-215-9
Hard cover, 780 pages
Publisher InTech
Published online 11, February, 2011
Published in print edition February, 2011

This book covers a number of developing topics in mass transfer processes in multiphase systems for a variety of applications. The book effectively blends theoretical, numerical, modeling and experimental aspects of mass transfer in multiphase systems that are usually encountered in many research areas such as chemical, reactor, environmental and petroleum engineering. From biological and chemical reactors to paper and wood industry and all the way to thin film, the 31 chapters of this book serve as an important reference for any researcher or engineer working in the field of mass transfer and related topics.

INTECH
open science | open minds

InTech Europe
University Campus STeP Ri
Slavka Krautzeka 83/A
51000 Rijeka, Croatia
Phone: +385 (51) 770 447
Fax: +385 (51) 686 166
www.intechopen.com

InTech China
Unit 405, Office Block, Hotel Equatorial Shanghai
No.65, Yan An Road (West), Shanghai, 200040, China
中国上海市延安西路65号上海国际贵都大饭店办公楼405单元
Phone: +86-21-62489820
Fax: +86-21-62489821

IntechOpen